Development of CFD Models for Mach 7 Ludwieg Tube Validation

Hayden A. Bilbo[1] and Christopher S. Combs[2]
The University of Texas at San Antonio, San Antonio, Texas, 78249, United States

A Mach 7 Ludwieg tube style wind tunnel has been designed and constructed at The University of Texas at San Antonio to perform research on hypersonic flow properties. In conjunction with experimental results being obtained from testing, computational fluid dynamic (CFD) models of the converging-diverging nozzle and a 15-degree half-angle wedge were developed in Ansys to compare to and validate this data. Steady state simulations were run for both models which relied on a k-ω turbulence model and a density-based solver. The simulations were simplified to 2D in order to minimize computational workload and solving time. The meshes were created in Ansys due to its wide range of powerful meshing tools and familiarity by the user, while the flows were solved for using Ansys Fluent. Bias values were implemented in the nozzle mesh to decrease element size towards the throat from the inlet and the outlet, and to decrease element size from the midplane to the outer wall. A bias was also included when meshing the wedge to create a smooth transition from the upstream mesh to the area above the wedge. Results from the nozzle simulations show a freestream Mach number of 7.05 and velocity of 736 m/s. These values fall reasonably close to the wind tunnels design specifications, which show a Mach number of 7.2 and velocity of 736 m/s. These results also display a similar boundary layer profile to that of particle image velocimetry (PIV) data obtained from experimentation. The wedge simulation results show a wave angle of roughly 22 degrees associated with the leading-edge oblique shock which was found to be the same value for schlieren images taken during testing. Both simulations result in very similar trends when compared to PIV and Schlieren data obtained from test campaigns, with the nozzle simulations also showing a strong parity with wind tunnel design parameters.

I. Introduction

A comprehensive study was conducted on The University of Texas at San Antonio's (UTSA) Mach 7 wind tunnel to validate computational models previously developed and to compare these results with experimental data. The newly constructed wind tunnel features a Ludwieg tube style design which consists of a long-tubed high-pressure chamber leading into the nozzle assembly. The wind tunnel was designed to operate at a Mach number of 7.2 and Reynolds numbers of up to 200×10^6 m^{-1} [1]. A method of characteristics code and computational fluid dynamics (CFD) were used in the initial design of the UTSA wind tunnel [2]. CFD studies have been performed in the past to assist with the design efforts of this facility [3,4] and are currently being employed and used as an extension for model comparison and potential first step in advisement for future test campaigns.

CFD studies in the hypersonic regime have steadily increased over the past decades [5,6]. Due to the inherent complexity of flow physics associated with this regime, several training and validation data sets are required to train CFD models to analyze intricate phenomena such as shock-wave/boundary-layer interactions [7,8], corner and juncture flows, and hypersonic flow separation amongst others. High mesh densities required for resolving boundary layer properties in hypersonic flows pose some limitations on these models such as simulating in 2D space to drastically reduce the requirements on computational resources and simulation time [9], or sacrificing on mesh quality in a high volume simulation. Two well-known programs often used to tackle these difficult tasks are Ansys and OpenFOAM. Ansys hosts an extensive suite of solvers with an intuitive interface, with OpenFOAM being an open-

[1] Undergraduate Research Assistant, Department of Mechanical Engineering, AIAA Student Member
[2] Dee Howard Endowed Assistant Professor, Department of Mechanical Engineering, AIAA Senior Member

source command line-based program which has a large set of steady state and transient flow solvers. Ansys was the program chosen for this analysis owing to its powerful but user-friendly interface and familiarity by the user.

This study relies heavily on the use of CFD to analyze hypersonic flow physics with velocity, pressure, Mach number, density, and temperature being key variables of interest. The first analysis conducted was a 2D Ansys nozzle simulation, also referred to as the wind tunnel simulation throughout this paper. The wind tunnel simulation was simplified to the nozzle region since this is the primary area of changing physics throughout the wind tunnel. Data obtained from a particle image velocimetry (PIV) test campaign were used to verify the boundary layer velocity profile and Mach number values. Another analysis was conducted on a 15-degree half-angle wedge, for which simulation data were compared to Schlieren images taken during wedge wind tunnel experiments. Ansys was also used here to model and simulate a 2D wedge which focused on the regions immediately left of and above the wedge surface. Images of density gradient were used to determine the oblique shock wave angle, which was then compared to the wave angle measured from the schlieren images. Analyzing the congruence between CFD and experimental results for these two cases provides a significant data set for validation of CFD models developed and increases confidence in experimental measurements.

II. Computational Approach

A. Wind Tunnel Simulation

The converging and diverging portions of the nozzle were simulated to gather data on key variables of interest and provide a glimpse of the operating conditions experienced in the test section. Ansys Fluent was used to simulate a 2D nozzle, using inlet and outlet pressures associated with the driver tube and vacuum tank wind tunnel pressures. The boundary conditions and simulation parameters used are as shown in Table 1.

Table 1. Boundary Conditions and Parameters of Ansys Wind Tunnel Simulation

Input Parameters	Values
Solver Type	Density-based
Solver State	Steady
Turbulence Model	k-ω SST
Inlet Pressure	Total Pressure of 2.07 MPa
Outlet Pressure	Static Pressure of 393 Pa
Inlet Temperature	297 K
Outlet Temperature	25.44 K
Outlet Height	101.6 mm
Throat Height	0.8052 mm

The values for pressure and temperature were chosen based on actual values seen in wind tunnel operation, providing a more direct comparison of computational results to wind tunnel experiments. The pressure and temperature inlet conditions correspond to the wind tunnel plenum conditions, whereas the outlet pressure and temperature are estimated to be equivalent to vacuum tank conditions. A density-based solver type was implemented due to its ability to account for compressibility effects at hypersonic flow velocities. The difference between this and the commonly used pressure-based solver is that density is calculated directly from the continuity equation, from which pressure can be found using the equation of state [10]. This approach is widely used for supersonic flow regimes which encounter large changes in density throughout the flow.

When generating the Ansys mesh, only half of the nozzle above the centerline axis was modelled since this line is a 2D axis of symmetry. Doing so greatly reduces the number of mesh elements and required computing time while providing increased mesh resolution capabilities. Sizing controls were also implemented at the inlet, symmetry plane, wall, and outlet edges to vary mesh size throughout the nozzle. The nozzle was split into two portions, the converging section and diverging section, to create mesh biases decreasing in size towards the throat. A bias was also used to decrease mesh size towards the nozzle wall, resulting in a wall mesh size of 8.9 μm near the throat and a total of 200,000 mesh elements. Figures 1 and 2 show the mesh in two different regions with included bias directions.

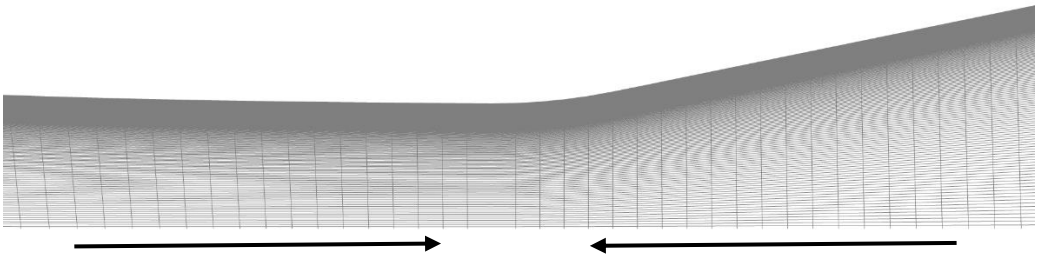

Fig. 1. Nozzle Mesh in Throat Region

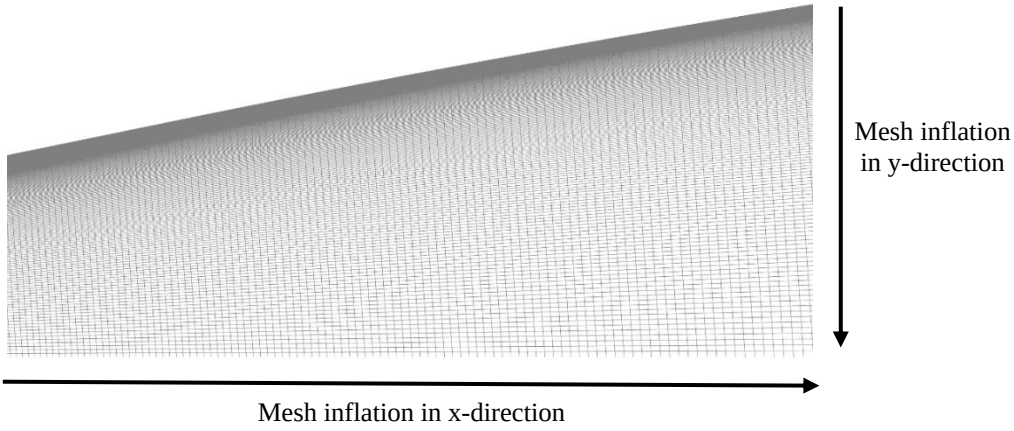

Fig. 2. Nozzle Diverging Section Mesh

B. Wedge Simulation

A wedge is a canonical geometry used in wind tunnel analysis with flow characteristics that are well defined in the literature [11,12]. The primary variables which govern the behavior of supersonic flow over a wedge are the turning angle (referred to as the half-angle in this study) and the upstream Mach number. The wedge was simulated with a 15-degree half-angle with a base length of 76.2 mm (3 inches). In order to reduce the computational time and simplify the geometry, only a small region in front of and above the wedge was modeled. A length scale of 76.2 mm (3 inches) in both regions was found to provide adequate room to ensure no flow restriction was taking place. An image of the mesh is shown in Fig. 3, which illustrates the bias created to minimize element size near the wedge leading edge. This bias was created to ensure a smooth transition from the upstream to downstream flow region through the geometry step change.

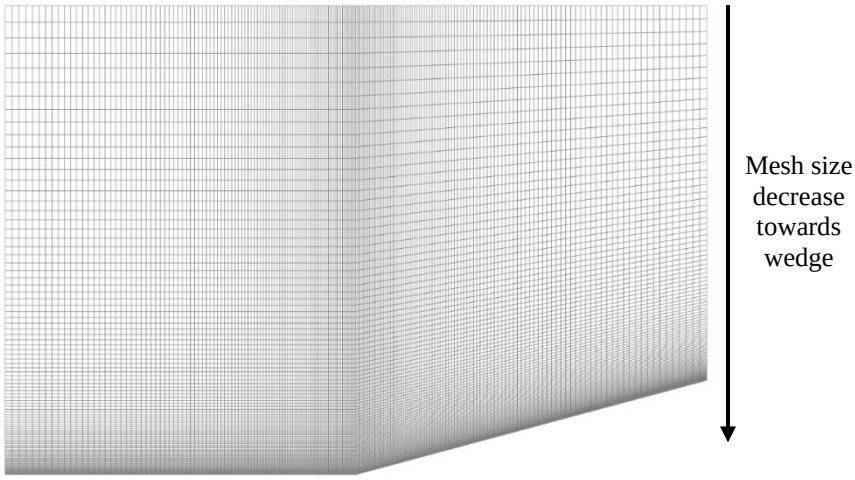

Fig. 3. Display of Mesh Created in Ansys

A different approach was taken when implementing the boundary conditions for this simulation. Since the Mach number had already been determined from wind tunnel CFD and experimental runs, this value along was used as a boundary condition imbedded in the far-field pressure input. The far-field pressure boundary includes the outer edges of the mesh excluding the bottom edge and wedge surface. Similar to the wind tunnel simulation, a symmetry condition was used for the bottom edge to simulate the mirror side of the test section. Finally, the wedge surface was simulated as an adiabatic wall with a no-slip condition. A summary of these conditions is show in Table 2.

Table 2. Wedge Simulation Boundary Conditions

Boundary	Value
Far-field Pressure	393 Pa
Bottom Edge	Symmetry
Wedge Surface	No-slip

III. Experimental Setup

A. Wind Tunnel

The wind tunnel experimental setup consists of the high-pressure driver tube, plenum, nozzle, test section, diffuser, and vacuum tank, respectively. The driver tube is the defining characteristic of a Ludwieg tube wind tunnel design and is the main component which differentiates it from a blow-down type of design. An image of the setup is shown in Fig. 4. This design and its construction are discussed extensively in Refs. [1-2,13].

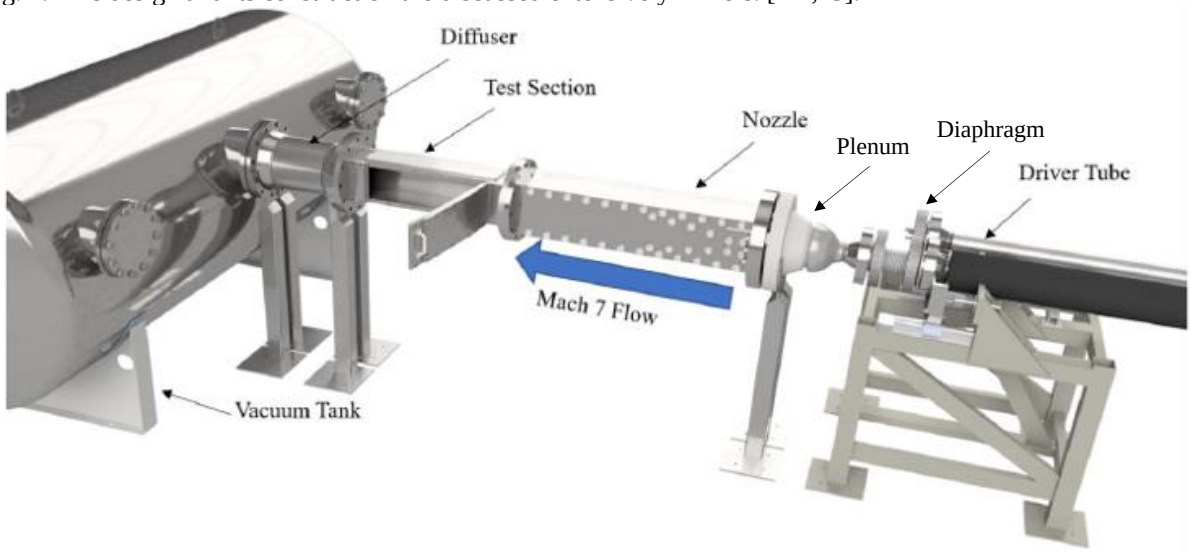

Fig. 4. Experimental Setup of Wind Tunnel [2].

The standard operating procedure is to first draw the vacuum tank down to around 350 Pa (0.05 psia), the lower limit of the vacuum pump used, after which the driver tube is pressurized using a compressor until the diaphragm bursts. The driver tube has a 101.6 mm (4 in) nominal diameter and is capable of operating at stagnation temperatures of up to 700 K and stagnation pressures up to 13.8 MPa (2000 psia). Typical burst pressures of the diaphragm are in the range of 1.90 – 2.24 MPa (275 - 325 psia). The test section has an area of 203.2 mm × 203.2 mm (8 in × 8 in) which was designed to provide a nominal Mach number of 7.2. At standard operating temperatures of 300 K, the test section is designed to run at a velocity of 736 m/s. This facility is coupled to several non-intrusive diagnostic equipment via the use of an in-house manufactured triggering circuit allowing the use of several laser and light-based diagnostic methods [14].

B. Particle Image Velocimetry

Particle image velocimetry (PIV) is an optical method of obtaining velocity data which utilizes high-powered lasers to scatter light off tracer particles seeded within in the air flow [15]. This technique is employed in several fluid dynamics campaigns to obtained quantitative information such as velocity, and shear stress pertaining to the flow field [16,17]. In this wind tunnel experiment, TiO2 was utilized as the seeding particle for the test gas which was air. The

second harmonic (532 nm) of a quasimodo pulse-burst Nd:Yag laser was formed into sheet of light to illuminate the particles. The scattered light from the laser was finally imaged on a Photron Fast Cam SAZ camera. Images from the PIV imaging were analyzed using the Davis 8.4 software developed by LaVision for PIV and the contours were obtained from the output velocity fields derived from the cross-correlation of the images. An image depicting PIV in a flow can be seen in Fig. 5.

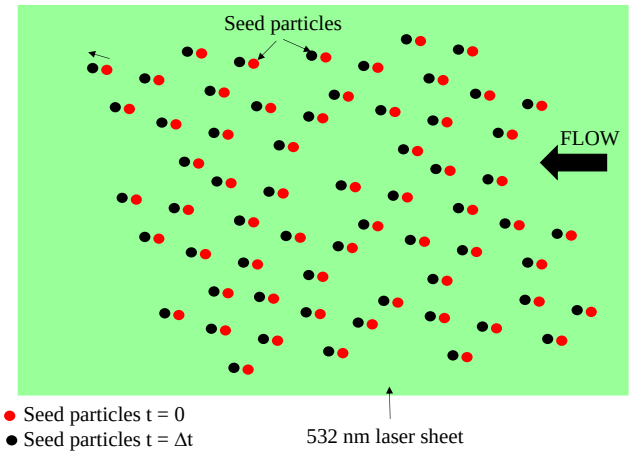

Fig. 5. Schematic of PIV.

C. Wedge Schlieren

Schlieren is an optical imaging technique which was used in the analysis of hypersonic flow over a wedge. This technique works by passing a collimated beam of light through the test section to collect density gradient information on the flow field. Two concave/spherical mirrors were used to collimate and then refocus the light before filtering via a knife edge. The knife edge blocks out half of the light and when implemented correctly produces density gradient information which is useful in visualizing shock waves produced in the flow. The knife edge was placed in a vertical position to filter out light in the horizontal direction. An image of the setup is shown in Fig. 6. A detailed description of schlieren imaging is given by [18].

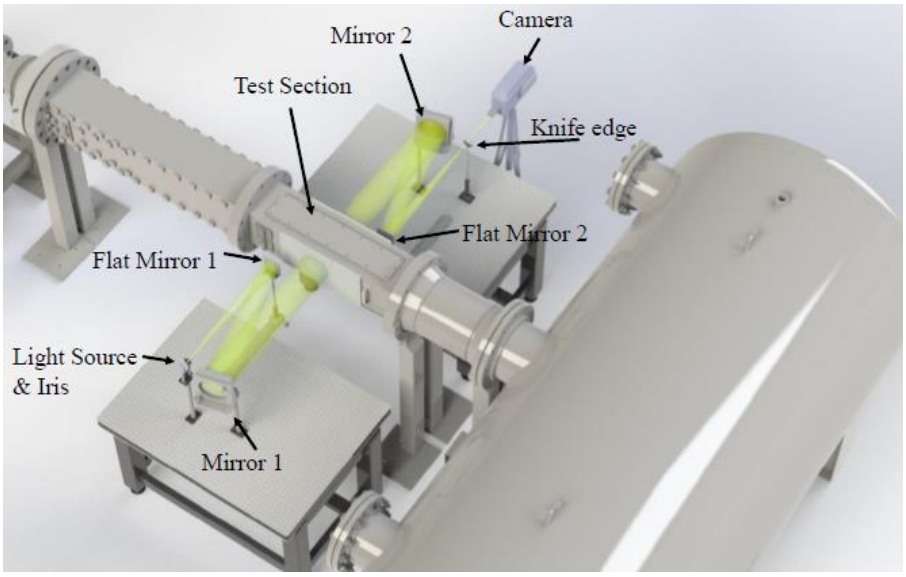

Fig. 6. Schlieren Imaging Setup of UTSA Wind Tunnel [1].

IV. Results

A. Wind Tunnel Simulation

The simulations ran on the entire nozzle produced results that aligned well with experimental measurements obtained from PIV. Figures 7-9 show some of the results obtained which illustrate Mach number, velocity, and static temperature distributions throughout the nozzle. Firstly, when comparing the CFD data to theoretical and experimental measurements, the Mach number of 7.05 (Fig. 7) obtained from Ansys was close but 2% below the value of 7.2 found in experiments. Although care was taken to ensure boundary conditions were consistent with the experimental setup, one source of this discrepancy could be slightly different operating conditions than what was simulated. Furthermore, the 2-dimensional nature of the simulation most likely impacted results as no 3-dimensional effects were considered in the solution. However, the considerably reduced run times observed when switching from 3D to 2D simulations makes this an effective method of quickly simulating wind tunnel conditions to within a reasonable margin of accuracy.

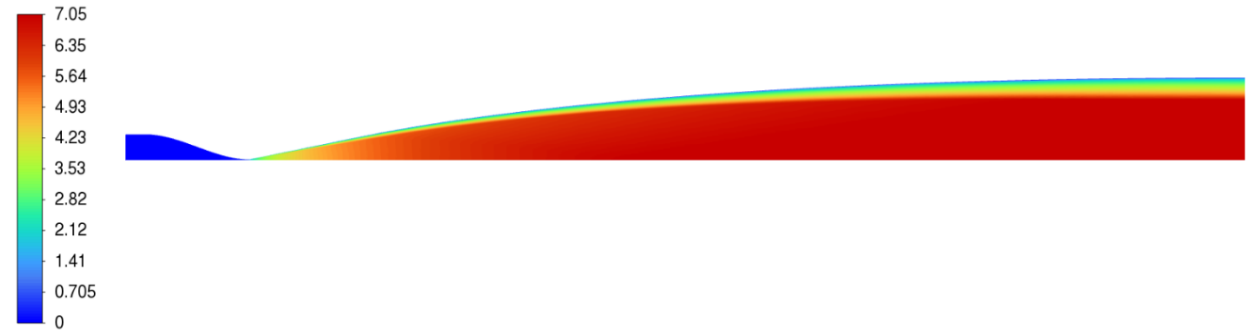

Fig. 7. Ansys Nozzle Mach Number Contour

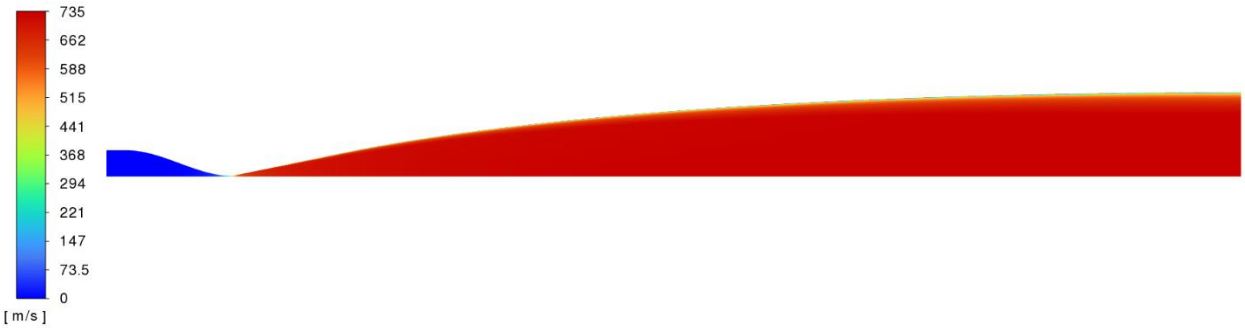

Fig. 8. Ansys Nozzle Velocity Contour

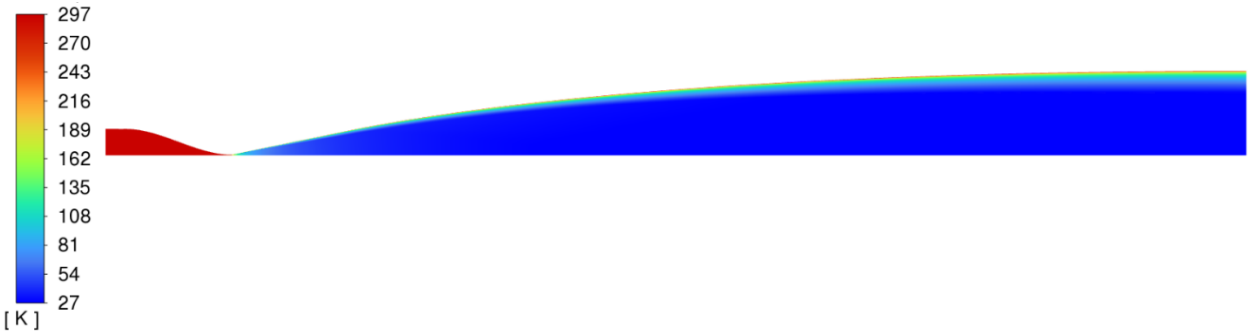

Fig. 9. Ansys Nozzle Static Temperature Contour

The density gradients shown in Fig. 10 indicate there is a standing shock wave located in the first part of the diverging portion which dissipates along the nozzle length towards the outlet. A reflected shock wave is also observed in the first third of the diverging nozzle which dissipates in energy with each reflection off the nozzle wall. Finally,

the large density gradient seen along the nozzle wall is an indication of where the boundary layer profile is located near the wall. This mainly serves as an illustration of the growing boundary layer size along the wall leading into the test section. Ansys density gradients helped in qualitatively inspecting the nozzle flow to find and correct geometry that led to shock waves in the facility.

Fig. 10. Ansys Nozzle Density Gradient Contour

The velocity boundary layer is a key flow characteristic that can be directly compared to PIV data obtained from experiments. A plot of the boundary layer velocity up until 18 mm is shown in Fig. 11, with a position of 0 mm indicating the nozzle wall. The saturated growth of velocity increase typically seen in nozzle flow is easily resolved in the simulation owing to the fine mesh which was used near the wall. In reality, the position dimension goes up to 101.6 mm, but even the shortened plot displays the velocity's trend up to its maximum value of 735 m/s. This maximum position value specified corresponds to the nozzle centerline at which the symmetry boundary condition is applied. From this analysis, a boundary layer height was calculated based on a δ_{99} criterion and this height was found to be 24.7 mm.

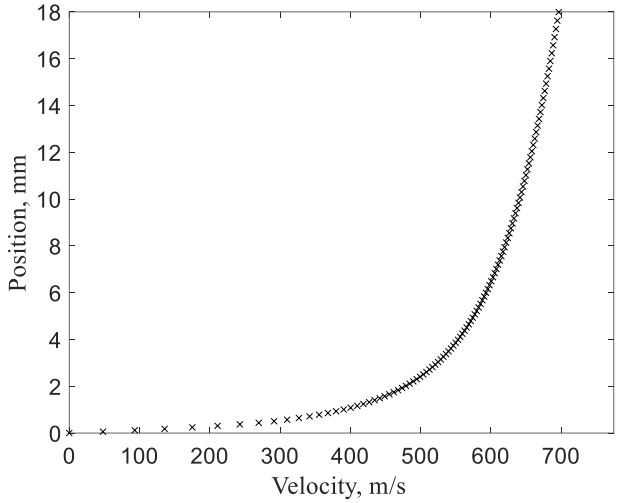

Fig. 11. Velocity Profile Obtained from Ansys Simulation

B. Wedge Simulation

The Ansys simulated wedge shows an oblique shock forming on the leading edge with an angle similar to that seen in the wedge schlieren images. The shock wave, which can easily be seen above the wedge surface in Figs. 12-14, can be analyzed using the density gradient as seen in Fig. 12. Using the upper line as a reference to track the shock wave, the wave angle is found to be roughly 22 degrees (measure relative to horizontal). This aligns well with oblique shock relations, which show that at a Mach number of 7.2 and turning angle of 15 degrees should produce a wave angle of 21.4 degrees. Considering that the angle was measured by hand in an image processing software, and that the precise wave angle is difficult to identify in practice, these values are well within the limits of uncertainty.

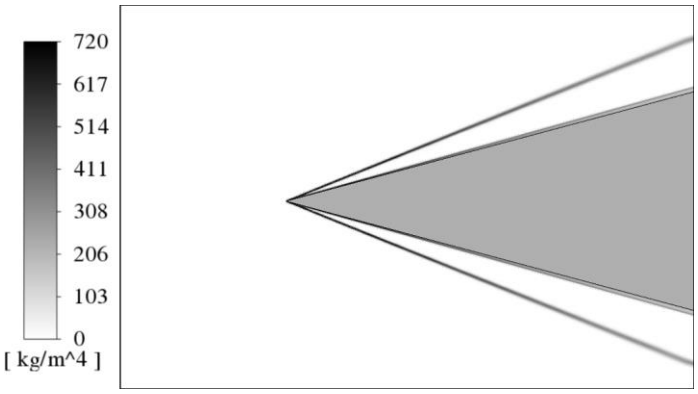

Fig. 12. Density Gradient of Simulated 15 Degree Half Angle Wedge

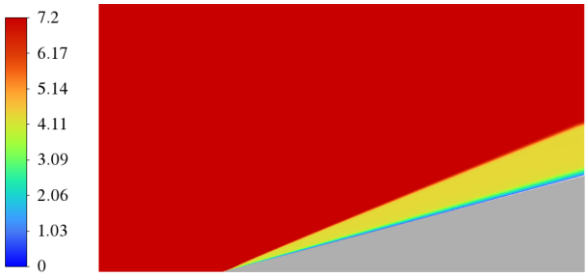

Fig. 13. Mach Number of Simulated 15 Degree Half-Angle Wedge

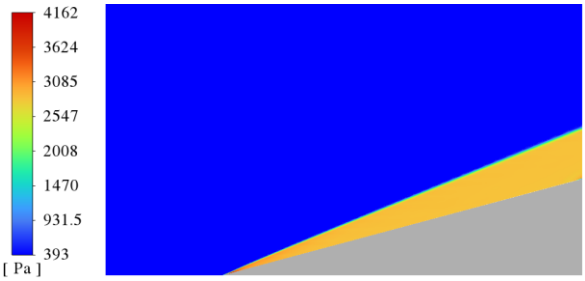

Fig. 14. Static Pressure of Simulated 15 Degree Half-Angle Wedge

C. Particle Image Velocimetry (PIV)

The primary results obtained from PIV experiments are velocity data of particles in the boundary layer region near the test section wall. The velocity boundary layer profile, with a starting data point at approximately 2 mm from the wall, is shown in Fig. 15. Although the resolution is not as high near the wall when compared to the wind tunnel simulations, the general shape of the profile is shown to align well between the two data sources. Furthermore, both profiles show a trend of velocity values towards the 736 m/s value which was calculated in the design and calibration stages of the wind tunnel [1].

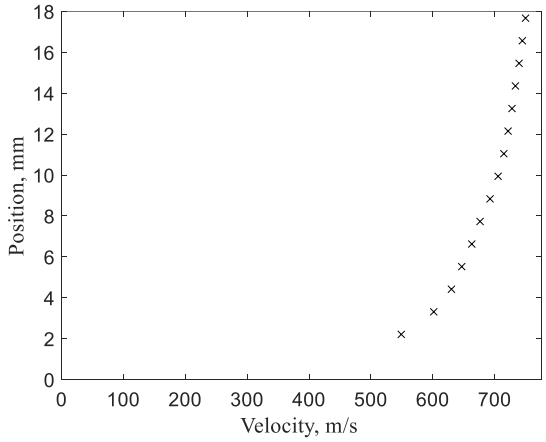

Fig. 15. Velocity Profile Obtained from PIV Analysis

D. Wedge Schlieren

Similar to what was seen in the simulated wedge results, the schlieren wedge images show a started hypersonic flow which reaches steady state conditions and produces a distinct oblique shock impinging on the wedge leading edge. The shock system, shown in Fig. 16, distinctly shows a steady oblique wave that has formed indicating a uniform

turning of the flow over the wedge. Moreover, a dark region of flow can be seen when looking at the region just above the wedge surface corresponding to the boundary layer profile. This profile does not show much growth along the wedge surface likely due to the lower flow velocities behind the shock and near the surface.

The wave angle was again measured by hand using software, which resulted in an approximate value of 22 degrees. This shows a strong correlation between these images and wind tunnel simulation results, which produced the same wave angle. This also indicates that the flow is indeed moving at a Mach number of around 7.2 as input in the Ansys wedge simulations.

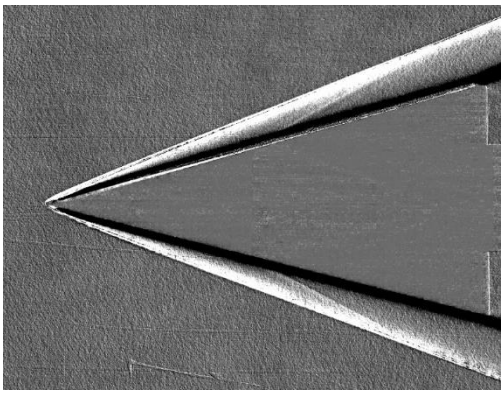

Fig. 16. Schlieren Images of 15 Degree Half Angle Wedge Test

E. Comparison of Ansys CFD and Experimental Results

Many similarities arise when comparing the wind tunnel computational results to theoretical design parameters and experimental measurements taken. First, the Mach number of 7.05 obtained from Ansys simulations was found to be similar to the value of 7.2 calculated in the wind tunnel's design. Discrepancies could be due to 3-dimensional flow effects that are not captured in the 2D simulation. Furthermore, the Ansys simulated velocity of 735 m/s corresponds very well to the value of 736 m/s, a difference of 0.1%, specified in the design phase [1].

As for comparison to the PIV results, the outlet boundary layer profile follows a similar trend to the PIV velocity results when plotted. The boundary layer profiles are both shown in Fig. 17, which shows the normalized velocity profiles with both normalized over their respective boundary layer heights.

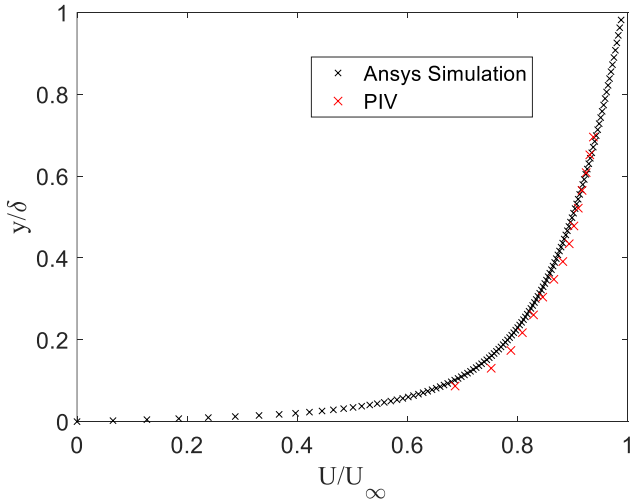

Fig. 17. Comparison of Ansys and PIV Boundary Layer Profiles.

Two points randomly selected in the flow field were used to compare velocity values obtained from PIV to those obtained from Ansys. Chosen data points were not at identical positions, so this is more of a general reference for comparison instead of a direct comparison between the data. All data points are shown in Table 3.

Table 3. Ansys and PIV Velocity Boundary Layer Values

Source	Position (mm)	Velocity (m/s)
Ansys Node 1	2.31	494.5
PIV Node 1	2.21	549.0
Ansys Node 2	7.75	617.3
PIV Node 2	7.73	676.3

The percent difference was calculated between each set of nodes, which came out to be 10% and 9% difference for nodes 1 and 2, respectively.

Comparing the Ansys wedge simulation to the schlieren imaging results, the wave angle measured was found to be nearly identical at 22 degrees. These measurements are subject to some variability due to the uncertainty in the exact points needed to measure the wave angle as well as user error in hand selecting the reference points. Nevertheless, visual comparison as shown in Fig. 18 and the estimated wave angle, which results in a Mach number close to 7, indicate agreeance with the simulated wedge and experiments conducted.

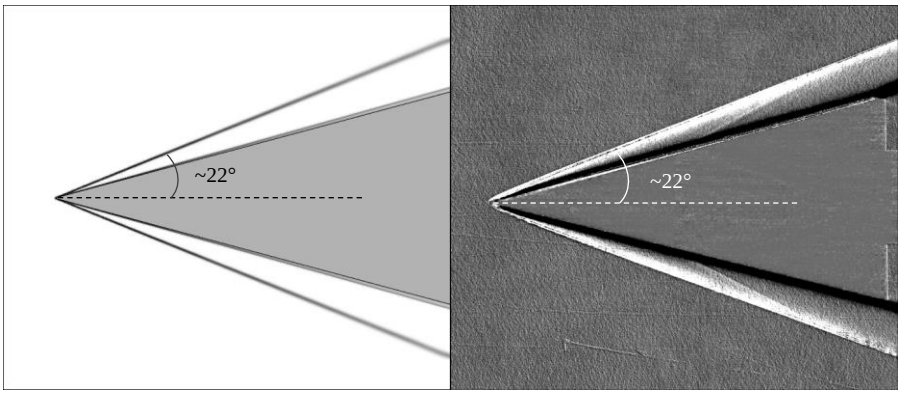

Fig. 18. Wedge Montage of Simulated Density Gradient (left) and Schlieren Image (right).

V. Conclusion

This paper presented a comparison of computational and experimental approaches to obtaining flow field data on UTSA's Mach 7 wind tunnel. The computational methods employed by Ansys were shown to agree quite well with test data gathered from wind tunnel runs conducted. The CFD Mach number results showed a slight deviation of 2% below the wind tunnel design Mach number. Potential for further work exists which could increase model accuracy by refining turbulence or solver parameters, both of which were set at default values for this analysis. Moreover, a 3D simulation could be employed to compare with 2D results obtained to quantify 3-dimensional effects on flow field variables of interest. OpenFOAM is a powerful open-source alternative to Ansys which could simulate these 3D effects; this software provides an opportunity for further refinement of simulation parameters and increased capabilities for parallel computing processes.

Acknowledgments

The authors would like to acknowledge Dr. Rodney Bowersox for providing the MOC code used in the development of the wind tunnel contour. The project was funded by …

References

[1] Hoffman, E. N. A., LaLonde, E. J., Delgado E., V., Chen, I., Bilbo, H. A., and Combs, C. S., "Characterization of the UTSA Mach 7 Ludwieg Tube," *AIAA SciTech 2022 Forum*, San Diego, CA, Jan. 2022. doi: 10.2514/6.2022-1600

[2] Hoffman, E. N. A., Bashor, I. P., and Combs, C. S., "Construction of a Mach 7 Ludwieg Tube at UTSA," *AIAA Aviation 2020 Forum*, June 2020. doi: 10.2514/6.2020-2998

[3] Bashor, I. P. and Combs, C. S., "RANS Simulations of the UTSA Mach 7 Ludwieg Tube."

[4] Bashor, I., Hoffman, E. N. A., Gonzalez, G., and Combs, C. S., "Design and Preliminary Calibration of the UTSA Mach 7 Hypersonic Ludwieg Tube," *AIAA Aviation 2019 Forum*, 2019, pp. 2859.
[5] Dolling, D. S., "Fifty Years of Shock-Wave/Boundary-Layer Interaction Research: What Next?," *AIAA Journal*, Vol. 39, No. 2001, pp. 1517– 1531.
doi: 10.2514/2.1476
[6] Knight, D. D., and Degrez, G., "Shock Wave Boundary Layer Interactions in High Mach Number Flows a Critical Survey of Current Numerical Prediction Capabilities," *AGARD Advisory Report Agard Ar., Tech. Rept. AR-319*, Vol. 2, 1998.
[7] Hoffman, E. N. A., Rodriguez, J. M., Cottier, S. M., Combs, C. S., Bathel, B. F., Weisberger, J. M., Jones, S. B., Schmisseur, J. D., and Kreth, P. A., "Modal Analysis of Cylinder-Induced Transitional Shock-Wave/Boundary-Layer Interaction Unsteadiness," *AIAA Journal* (2021): 1-19.
[8] Lindörfer, S. A., Combs, C. S., Kreth, P. A., and Schmisseur, J. D., "Numerical Simulations of a Cylinder-Induced Shock Wave/Boundary Layer Interaction," *55th AIAA Aerospace Sciences Meeting*, AIAA Paper 2017-0534, Jan. 2017.
doi: 10.2514/6.2017-0534
[9] B. Zang, U. S. Vevek, and T. H. New, "OpenFOAM based numerical simulation study of an underexpanded supersonic jet," *55th AIAA Aerospace Sciences Meeting*, Jan. 2017.
doi: 10.2514/6.2017-0747
[10] Fluent, I.N.C. "FLUENT 12.0 user's guide" *Fluent documentation (2009).*
[11] Orlik-Ruckemann, K.J., "Effect of wave reflections on the unsteady hypersonic flow over a wedge," *AIAAJ*, vol. 4, no. 10, Oct. 1966.
doi: 10.2514/3.3813
[12] Rodkiewicz, C. M., "Hypersonic Flow with Viscous Interaction over a Sharp Slender Wedge," *AIAAJ*, vol. 12, no. 1, Jan. 1974.
doi: 10.2514/3.49143
[13] Hoffman, E. N. A., Rodriguez, J. M., Garcia, M., Delgado E., V., LaLonde, E. J., and Combs, C. S., "Preliminary Testing of the UTSA Mach 7 Ludwieg Tube," In *AIAA AVIATION 2021 FORUM*, 2021, pp. 2979.
[14] LaLonde, E. J., Delgado E., V., and Combs, C. S., "Development of High-Speed Data Acquisition Triggering System for Hypersonic Wind Tunnel Applications," *AIAA Region III & IV Student Conference*, 2021.
[15] Melling, A. "Tracer particles and seeding for particle image velocimetry," *Measurement science and technology 8*, no. 12 1997: 1406.
[16] Anwar, M., "Setup of Particle Image Velocimetry (PIV) in Hypersonic Flows," 2008.
[17] Schreyer, A.-M., Sahoo, D., Williams, O. J. H., and Smits, A. J., "Experimental Investigation of Two Hypersonic Shock/Turbulent Boundary-Layer Interactions," *AIAA Journal*, Vol. 56, No. 12, 2018, pp. 4830-4844.
[18] Settles, G. S., "Schlieren and shadowgraph techniques: visualizing phenomena in transparent media," *Springer Science & Business Media*, 2001.